



Trade Science Inc.

ISSN : 0974 - 7486

Volume 8 Issue 12

Materials Science

An Indian Journal

Full Paper

MSAIJ, 8(12), 2012 [493-502]

Effect of blend ratio on thermal and optical properties of poly (methyl methacrylate)/poly (vinyl acetate) films

F.H.Abd-El Kader, W.H.Osman, R.S.Hafez*

Cairo University, Faculty of Science, Department of Physics, (EGYPT)

E-mail: R.S_Hafez@yahoo.com

Received: 22nd May, 2012 ; Accepted: 2nd October, 2012

ABSTRACT

Films of poly (methyl methacrylate) / Poly (vinyl acetate) (PMMA/PVAc) with different concentrations were prepared by using cast technique. The samples were investigated by differential thermal analysis (DTA), thermogravimetric analysis (TGA) and UV/visible spectra. A single glass transition temperature for each blend was observed in DTA thermograms, which reflects the existence of miscibility of such system. Thermogravimetric characterization and the calculated values of activation energies revealed that the blend sample of 75 wt% PVAc content has a more thermal stability than the other blends. The variation of band tail energy with the composition of the blend indicated that the model based on electronic transitions between localized states is preferable. The refractive index dispersion curves were simulated by both Cauchy and single effective oscillator models. The calculated color parameters such as L^* , U^* , V^* , and C^* for 25 wt% PVAc blend sample were found to be dependent on addition of malachite green and γ -irradiation. © 2012 Trade Science Inc. - INDIA

KEYWORDS

Thermal analysis;
Optical parameters;
 γ -irradiation;
Malachite green;
Color detection.

INTRODUCTION

Polymer blends often exhibit properties that are superior compared to the properties of the parent polymers^[1-3]. The properties of the final product vary according to the blend composition, and whether the material is subjected to further addition of dye substances or exposure to γ -radiation. Identifying the effect of such parameters makes it easy to modify the blend system to meet performance and cost objectives as required for new and changing markets^[4,5].

PMMA is an organic amorphous thermoplastic which is optically transparent, hard, and rigid; therefore

it has been widely used in the construction of a variety of optical devices, such as optical lenses. Also, it is used in medical applications, particularly for hard tissue repairs and regeneration^[6]. However, PMMA has poor thermal stability that restrains it from applications at high temperature^[7]. One possible solution to address this problem is to blend PMMA with another polymer of relatively high thermal stability such as PVAc. PVAc belongs to the group of polymers that are of special technological interests and hence has been used in many domestic and commercial everyday applications. PVAc also acts as a stabilizer with respect to thermal and photochemical degradation when the process takes place

Full Paper

in air^[8]. PMMA and PVAc make an important pair of polymers where their properties are complimentary and could be used to form improved enhanced blends.

Organic dyes are commonly added into polymer blends as a soluble color concentrates where they scatter no light and display excellent transparency. Recently, dye-polymer composites have received considerable attention as potential electro-optic materials^[9]. Blend properties could be improved further by subjecting samples to γ -irradiation. Polymer materials are susceptible to radiation and affected by it where many properties such as structural, optical, thermal, electrical and mechanical properties can be altered^[10]. Such changes are attributed to the chemical bond scissions and/or cross-linking induced by high-energetic radiation.

The aim of the present work is to perform a study on the effect of composition ratio on thermal and optical properties of PMMA/PVAc wt/wt% blends. The dispersion behavior of refractive index for the produced samples is discussed through the application of Cauchy and single effective oscillator models. Also, the effect of both γ -irradiation and malachite green additive on the color parameters of 25 wt% PVAc content in blend samples were discussed.

EXPERIMENTAL

Polymer specimens used in this study were synthetic polymers. PMMA $[C_5O_2H_8]_n$ was supplied by Aldrich Co. Its molecular weight is approximately 120,000. PVAc $[C_4H_6O_2]_n$ was supplied by Acros Organics, USA. Its molecular weight is approximately 170,000. A dye called malachite green $[C_{23}H_{25}ClN_2]$ was obtained from Cambrian Chemicals.

The PMMA/PVAc films were prepared by dissolving the two polymers in chloroform then, casting the blends onto stainless steel Petri-dishes where they were left to dry at room temperature for about 24h until the solvent has completely evaporated. Samples of different blend concentration 100/0, 75/25, 50/50, 25/75 and 0/100 wt/wt % PMMA/PVAc were produced. Malachite green of concentration 0.05 wt % was added only to the mixed solution of 75/25 wt/wt % PMMA/PVAc and the steps to form the film were similar to the previous samples. The sample of 75/25 wt/wt % PMMA/PVAc undoped and doped with malachite

green were irradiated by different γ -doses in the range from 5 up to 100kGy using ^{60}Co source with a dose rate of 8.6kGy/h at room temperature.

Thermal analysis was carried out using a computerized differential thermal analysis and thermogravimetric analysis manufactured by Shimadzu 60H, Japan (DTG). All tests were carried out under nitrogen atmosphere 30 ml/min and a heating rate of 10 °C/min. The UV/visible absorption of the samples was performed using a Perkin Elmer 4 β spectrometer over the wavelength range from 200 up to 800 nm. For irradiated specimens measurements were carried out 24h after irradiation and performed several times until reproducible results were obtained. The tristimulus transmittance values (X, Y, Z) were calculated using the transmittance data obtained in the visible range according to the CIE system^[11]. Also, the CIE three-dimensional color constants (L^* , U^* , V^*), chroma (C^*) and color difference (ΔE) were evaluated.

RESULTS AND DISCUSSION

Differential thermal analysis (DTA)

Figure 1 shows the DTA diagrams for PMMA, PVAc homopolymers and their blends of concentrations 75/25, 50/50 and 25/75 wt/wt% PMMA/PVAc in the temperature range from 30 up to 400 °C. The DTA thermogram for pure PMMA shows three endothermic phase transitions at around 110 °C, 302 °C and 372 °C. The first endothermic phase transition is shallow and broad and could be assumed to be the glass transition temperature (T_g) which is close to those published in the literature^[12-13]. The other two peaks are due to the high molecular weight of PMMA and are attributed to the disentanglements of the high molecular weight chain^[14]. On the other hand DTA thermogram for pure PVAc shows two shallow endothermic peaks at 46 °C and 310 °C, and one exothermic peak at 339 °C. The first endothermic peak is attributed to the glass transition temperature, which is slightly higher than that previously reported^[15-17]. The second phase transition may be due to the thermal degradation process. However, the latter exothermic phase transition is due to the evolution of acetic acid^[18]. PMMA and PVAc, as well as blends were considered to be completely amorphous because of the absence of the melting peak

in their thermograms^[19].

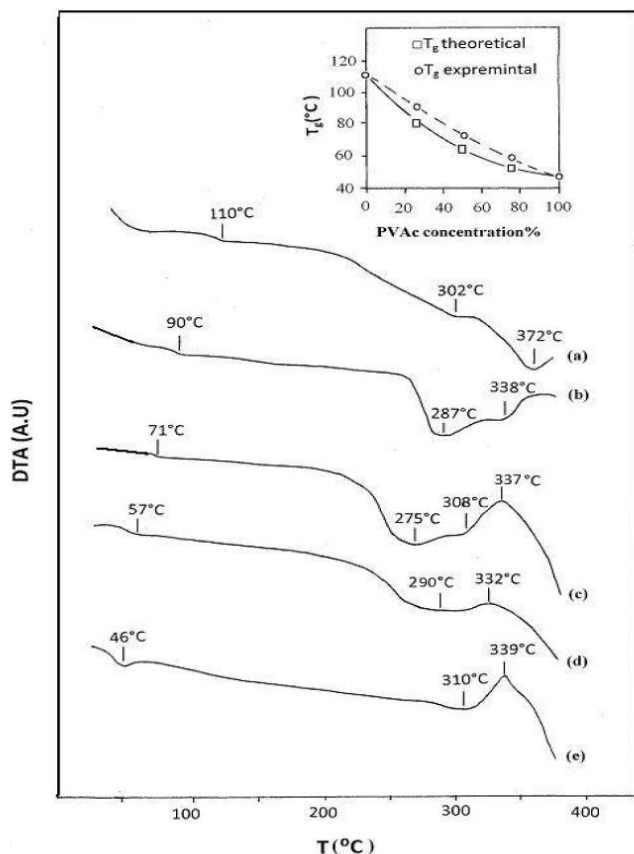


Figure 1 : DTA diagram for PMMA/PVAc blend samples; (a) 100/0, (b) 75/25, (c) 50/50, (d) 25/75 and (e) 0/100 (wt/wt%)

When considering the blend samples results, each blend shows a single glass transition peak with its position lying between those of the two pure polymers. It is observed that the values of T_g for all blends decreased with increasing the PVAc content. The existence of a single T_g reveals that the blend samples were miscible through all composition ratios^[13,19]. The DTA curves of the 25 and 50 wt% PVAc samples show two independent endothermic peaks in the temperature range 250 – 350 °C, while for the 75 wt% PVAc sample the two endothermic peaks appeared overlapping each other, as seen in Figure 1. These endothermic peaks of the blend samples are deeper than those of the pure PMMA and shifted towards lower temperatures. The characteristic exothermic peak in the DTA curve of PVAc still appeared in blends with 50 and 75 wt% PVAc but disappeared for 25 wt% PVAc sample.

The inset in Figure 1 shows the relationship between the T_g values and PVAc content for the investigated samples. The dashed line represents the experimental

values of T_g that was obtained from the DTA thermograms and the solid line represents the theoretical values of T_g calculated from the following equation which was introduced by Fox^[20]

$$1/T_{g(\text{blend})} = (W_1/T_{g1}) + (W_2/T_{g2}) \quad (1)$$

where W_1 and W_2 are the weight fractions and T_{g1} and T_{g2} are the respective glass transition temperatures of the homopolymers. The experimental data of T_g for the blends do not appear to follow the calculated theoretical values by Fox rule quite well. The deviations are in the range 5 to 8 % for all blends and the experimental T_g values are somewhat higher than the ideal values exhibiting positive deviation. This shows that it is plausible to consider that there is a limited miscibility between PMMA and PVAc homopolymers in the full composition range.

Thermogravimetric analysis (TGA) and its derivative (D_rTG)

Figure 2 presents the TGA and D_rTG thermograms of PMMA, PVAc homopolymers and their blend samples at temperatures up to 400 °C. Three stages of thermal decomposition are clearly seen for pure PMMA. The first stage is at T_{max} equals to 169 °C (temperature where decomposition rate is maximum) which corresponds to the depolymerization initiated by weak head-to-head linkages together with weak peroxides and/or hydroperoxides linkages^[7,21,22]. However, in this stage the weight loss was found to be equal to 10.08 wt %, suggesting that there are a few of such linkages. In the second stage T_{max} equals 287 °C, which is a result of radical transfer to unsaturated chain ends and in the third and final stage T_{max} equals 380 °C which indicates random scission^[23,24]. The DTA curve for pure PMMA showed similar behavior through the decomposition process as previously stated. However, the TG thermogram of PVAc shows that it has undergone a one-step into the degradation process at temperatures between 300 °C and 400 °C with T_{max} equal 345 °C. PVAc and 75 wt% PVAc blend sample, show that they are stable up to 300 °C and 245 °C respectively, and nearly no loss in weight was observed, but other samples show stability up to 100 °C only. This difference in the thermal stability of the individual polymers is related to the structure of the polymers. For example, the acetate groups in PVAc are attached through C-O bonding,

Full Paper

while the acrylate groups in PMMA are attached through C-C, the latter possesses relatively lower dissociation energy. As seen in Figure 2 there are three stages of thermal decomposition for 25 wt% and 50 wt% PVAc blend samples while only two stages were found for the 75 wt% PVAc blend sample. In addition, the percentage weight loss for 75 wt% PVAc content in the second stage is lower than the pure PMMA and other blend samples. These results indicate that the thermal stability of the blend samples increase with increasing PVAc content at temperature range from ambient temperature up to 300 °C. The temperature range of decomposition, the percentage weight loss in each degradation step for homopolymers and their blends are given in TABLE 1.

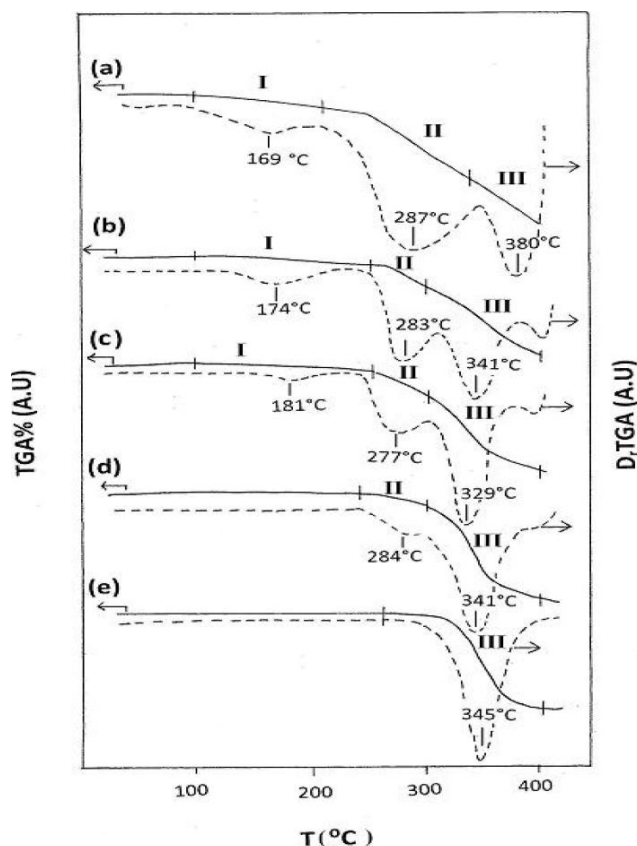


Figure 2 : TGA and D₁TGA for PMMA/PVAc blend samples; (a) 100/0, (b) 75/25, (c) 50/50, (d) 25/75 and (e) 0/100 (wt/wt%)

The general kinetic equation of a solid-state decomposition reaction is given as follows^[25]:

$$d\delta/dt = A f(\delta) \exp(-E_a/RT) \quad (2)$$

where $\delta = (w_0 - w_t) / (w_0 - w_\infty)$ is the fractional reaction, w_0 is the initial weight and w_∞ is the weight at the end of the

TABLE 1: TG and D₁TG data for PMMA/PVAc wt/wt % blend samples

PMMA/PVAc wt/wt %	Degradation process	Transition temperature (°C)*			Weight loss (%)
		T _i	T _{max}	T _c	
100/0	I	101	169	210	10.08
	II	210	287	300	56.90
	III	300	380	400	30.08
75/25	I	100	174	210	5.27
	II	230	283	295	22.49
	III	300	341	400	54.38
50/50	I	102	181	189	4.03
	II	239	277	294	18.70
	III	294	329	400	59.01
25/75	I	-----	-----	-----	-----
	II	245	284	300	15.03
	III	300	341	400	70.08
0/100	I	-----	-----	-----	-----
	II	-----	-----	-----	-----
	III	300	345	400	74.01

*T_i, temperature at which decomposition starts; T_{max}, temperature at which decomposition rate is maximum; T_c, temperature at which decomposition is completed

experiment and w_t is an actual weight at time t ; $f(\delta) = (1 - \delta)^m$ is the kinetic model function in a differential form; m is the reaction order; E_a is the activation energy; R is the gas constant; T is the temperature in Kelvin and A is the pre-exponential factor in the Arrhenius equation.

Various methods have been jointly employed to calculate the activation energy and determine the decomposition mechanisms. In this work, the Coats-Redfern (CR) and Horowitz-Metzger (HM) methods were used to calculate the activation energy of pure polymers and their blend samples.

The Coats-Redfern^[25] method is based on the following equation for studying thermal degradation kinetics at order $m=1$;

$$\ln[-\ln(1-\delta)/T^2] = \ln[(AR/\phi E_a)(1-2RT/E_a)] - E_a/RT \quad (3)$$

where ϕ is the heating rate. By plotting $\ln[-\ln(1-\delta)/T^2]$ versus $1000/T$ we get a straight line with a slope equals to $(-E_a/R)$.

The other method that proposed by Horowitz-Metzger^[26] is described by the following equation:

$$\ln[-\ln(1-\delta)] = E_a \theta / RT_s^2 \quad (4)$$

In this method, $\ln[-\ln(1-\delta)]$ is plotted versus $\theta = (T - T_s)$, in which T_s is the temperature of maximum degradation, resulting in a straight line whose slope is E_a/RT_s^2 .

The calculated activation energy (E_a) values accord-

ing to both models are given in TABLE 2. It is found that the E_a values calculated by both CR and HM methods are relatively nearly close to each other and have the similar trend for all decomposition regions. Thus, both CR and HM relations are suitable for understanding the kinetics of the thermal decomposition of the present samples. It is clear that the second stage showed higher activation energies when compared with first and third stages for blend samples. Also, in the second stage the E_a values for 75 wt% PVAc blend sample is higher than those of other composition ratios which reflect its higher bond strength. The E_a values in the third stage for blends lie in the intermediate values between those of pure polymers.

TABLE 2 : Activation energies calculated by Coats-Redfern (CR) and Horowitz-Metzger (HM) methods for PMMA/PVAc wt/wt% blend samples

PMMA/PVAc wt/wt %	Degradation process	(CR)	(HM)
		E_a (kJ/mole)	E_a (kJ/mole)
100/0	I	58.83	66.84
	II	40.09	51.15
	III	169.95	178.84
75/25	I	44.64	56.68
	II	190.60	192.77
	III	84.89	94.04
50/50	I	46.25	58.27
	II	194.14	197.76
	III	82.27	87.45
25/75	I	-----	-----
	II	200.58	204.89
	III	78.24	81.63
0/100	I	-----	-----
	II	-----	-----
	III	174.27	181.00

Optical spectroscopy in UV-visible range

Figure 3 depicts the UV-visible spectra of both PMMA and PVAc homopolymers as well as their blends 75/25, 50/50 and 25/75 wt/wt% PMMA/PVAc in the wavelength range from 200 up to 700 nm. The general characteristic of all absorption spectra are composed of an almost flat base line (absorption negligible) and a steep rise near the absorption edge (remarkable absorption). The absorption spectra of PMMA and PVAc homopolymers contain an intense band at 230 and 227 nm respectively, which are due to the presence of chromophoric groups. However, for the blend samples the band position shifted to lower wavelength with increas-

ing PVAc content in the system. This shift indicates the formation of intermolecular interaction between PMMA and PVAc. Also, Figure 3 showed that the blend sample of 75 wt% PVAc gave the highest absorbance value while the blend sample of 25 wt% PVAc showed the lowest absorbance value in the UV wavelength range. It should be noted that there are no absorption bands in the visible region for all the samples being investigated because the films are transparent.

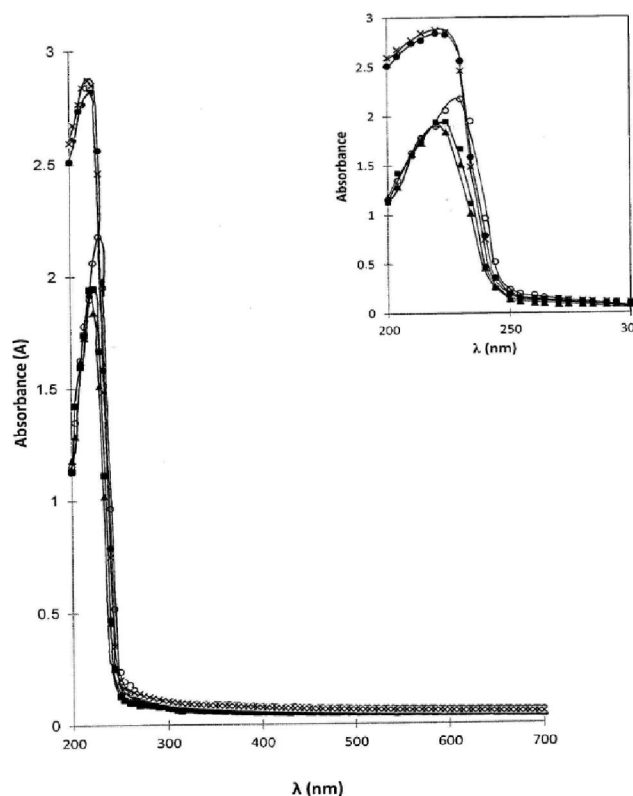


Figure 3 : Absorption spectra for: (o) 100/0, (▲) 75/25, (●) 50/50, (x) 25/75 and (■) 0/100 PMMA/PVAc (wt/wt%) blend samples

(a) Optical parameters

The absorption coefficient $\alpha(\nu)$ can be directly determined from the optical absorption spectra relation; $\alpha = 2.303(A/d)$ where A is the absorbance and d is the thickness of the sample. The calculated values of the absorption coefficient are relatively small (~ 50 - 1800 cm^{-1}) which are similar to those of most-carrier concentration of amorphous materials. Therefore, the samples under investigation are considered weakly absorbing. A plot of the absorption coefficient against the photon energy for both PMMA and PVAc homopolymers and their blend samples are shown in Figure 4a. It is clear that there is no sharp absorption edge which is

Full Paper

a characteristic of the glassy state of the material. The data points show a linear dependency between the absorption coefficient and the photon energy near the band edge. The absorption edge; which is the value of the photon energy at zero absorption, is obtained by the extrapolation of the linear relationship to zero absorption, i.e. the absorption edge is the intercept with the x-axis. The values of the absorption edge for the blend samples are nearly equal and lie at 5.05 within an experimental error of ± 0.05 . This equality indicates that there is no variation in the optical band gap energy in the blend system^[4].

The absorption edge as described for many amorphous materials, most commonly, follows the Urbach equation^[27];

$$\alpha = \alpha_0 \exp(h\nu/E_e) \quad (5)$$

where α_0 is constant and E_e is the width of the tail of localized states in the band gap. Figure 4b shows the relation between $\ln \alpha$ and $h\nu$ for the PMMA and PVAc homopolymers, and their blend samples. The straight line representations of the data suggest that the absorption follows the quadratic relation for inter-band transition^[28] and hence satisfies the Urbach rule. The values of band tail E_e were calculated from the slopes of these lines, which are found to be 1.30, 1.79, 1.40, 1.64 and 1.88 at 100/0, 75/25, 50/50, 25/75 and 0/100 wt/wt% PMMA/PVAc samples respectively. However, E_e vary remarkably with the composition of the blend; hence the model based on electronic transitions between localized states is preferable to this case^[29-31].

The refractive index (n) is another important parameter here, if multiple reflections are neglected, reflectance (R) is obtained from the transmittance (T) data using the following relation:

$$R = 1 - [T \exp(\alpha d)]^{1/2} \quad (6)$$

Also, the reflectance of light is described by Fresnel equation as follow;

$$R = \frac{(n-1)^2 + K^2}{(n+1)^2 + K^2} \quad (7)$$

where K is the extinction coefficient; $K = \alpha \lambda / 4\pi$ where λ is the wavelength. For infinitely small values of K , equation (7) reduces to that for a normal insulator;

$$n = \frac{(1+R^{1/2})}{(1-R^{1/2})} \quad (8)$$

The dispersion spectra of the refractive index given in Figure 5 were interpolated to fit the Cauchy formula^[32];

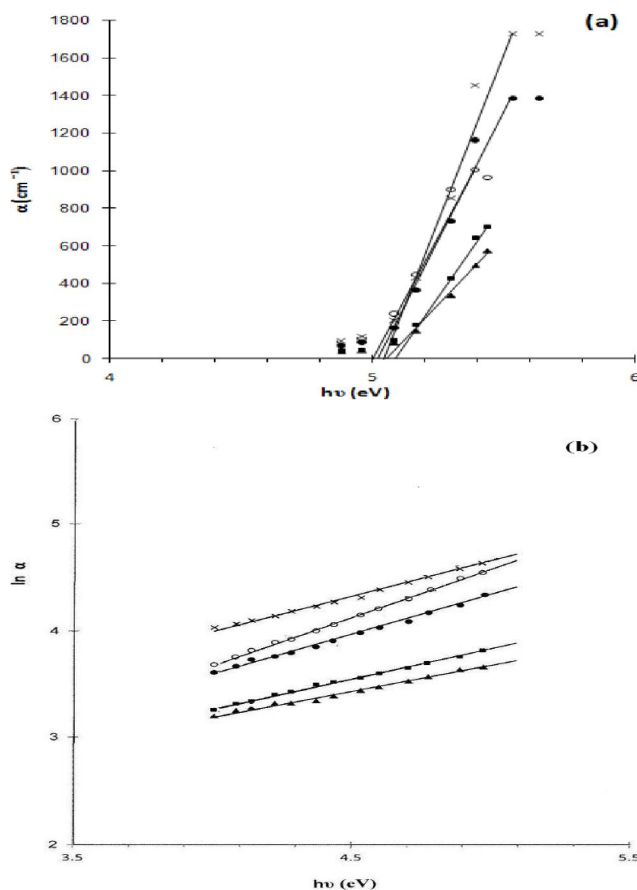


Figure 4 : Relation between absorption coefficient (a) & $\ln \alpha$ (b) as a function of photon energy for: (o) 100/0, (\blacktriangle) 75/25, (\bullet) 50/50, (\times) 25/75 and (\blacksquare) 0/100 PMMA/PVAc (wt/wt%) blend samples

$$n = \delta + (\beta/\lambda^2) \quad (9)$$

where δ and β are the Cauchy's parameters. For $\lambda \rightarrow \infty$ i.e. $\nu \rightarrow 0$ hence $\delta \rightarrow n_0$. The values of n_0 for homopolymers PMMA and PVAc are 1.49 and 1.40 respectively. The value of n_0 for PMMA is in agreement while for PVAc appears slightly different than those reported in the literature^[4,33,34-36]. The refractive indices values for the blend samples are found to be 1.42, 1.47 and 1.43 for 75/25, 50/50, 25/75 wt/wt% PMMA/PVAc respectively. These values did not vary proportionally to the composition ratio but they lie between the two values of the homopolymers. In general, the change in the refractive index could be attributed to various factors including crystallinity, density, electronic structure and defects. The compositional dependency of n_0 may be caused by the interface phenomena due to domain structure, molecular orientations and processing conditions^[37].

The single oscillator model is used for the simula-

tion of the results, it was developed by Wemple and DiDomenico^[38,39] and it suggests that the data could be described by:

$$n^2-1 = E_d E_0 / (E_0^2 - E^2) \quad (10)$$

where E_0 is the average excitation energy for electronic transitions and E_d is the dispersion energy which is a measure of the strength of the interband optical transitions. Equation (10) is presented graphically in Figure 6 where the values for the dispersion parameters E_0 and E_d are determined and also given in TABLE 3. The values of both E_0 and E_d vary but, in general, not proportional to the blend composition ratio.

The refractive index at zero-frequency (n_0) and average wavelength (λ_{os}) of samples can be obtained using the Sellmeier oscillator representation^[40]:

$$(n_0^2 - 1) / (n^2 - 1) = 1 - (\lambda_{os} / \lambda)^2 \quad (11)$$

Substituting for the oscillator strength; $S_{os} = (n_0^2 - 1) / \lambda_{os}^2$ and rearranging equation (11) gives;

$$(n^2 - 1)^{-1} = (1 / S_{os} \lambda_{os}^2) - (1 / S_{os} \lambda^2) \quad (12)$$

The oscillator parameters were calculated by fitting the

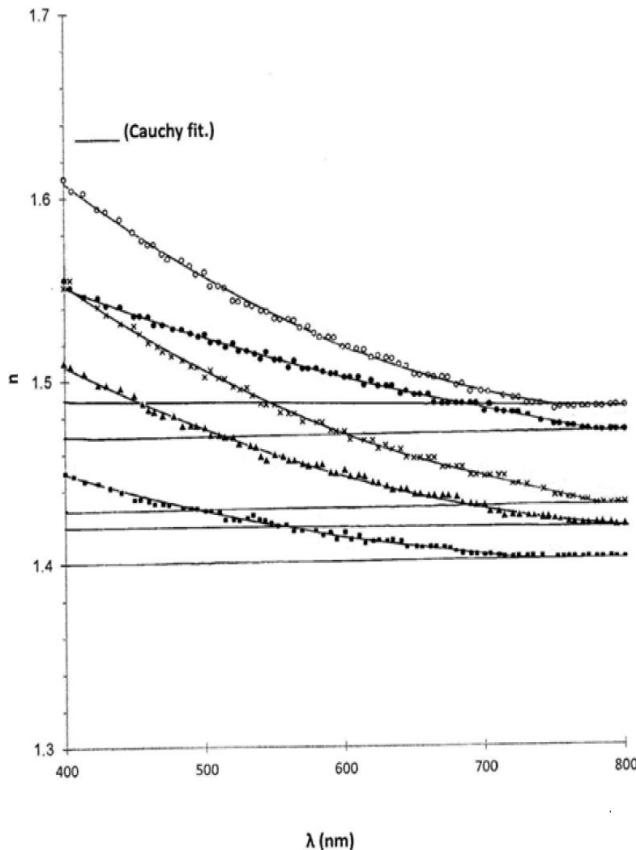


Figure 5 : Variation in refractive index with wavelength for: (o)100/0, (▲) 75/25, (■) 50/50, (x) 25/75 and (●) 0/100 PMMA/PVAc (wt/wt%) blend samples

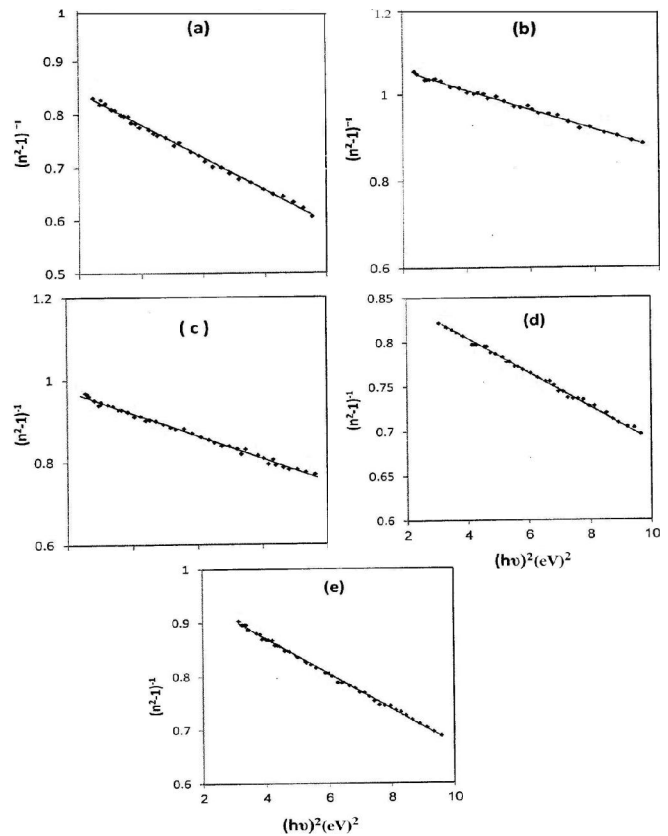


Figure 6 : Relation between $(n^2-1)^{-1}$ vs $h\nu^2$ for: (a) 100/0, (b) 75/25, (c) 50/50, (d) 25/75 and (e) 0/100 (wt/wt%) PMMA/PVAc blend samples

data into a linear function of $(n^2-1)^{-1}$ versus λ^{-2} . By using the slope and intercept of the straight line interpolation, the values of the parameters λ_{os} and S_{os} are determined. All parameters associated with this effective oscillator model are listed in TABLE 3. It was observed that the obtained values of the oscillator strength for the blend samples were of the same order of magnitude as those obtained for pure homopolymers. A comparison between the values of n_0 obtained by using Cauchy and single effective oscillator methods show that there is a good agreement between these models.

TABLE 3 : The single-oscillator parameters for PMMA and PVAc homopolymers and their blend samples

PMMA/PVAc wt/wt%	E_0 (eV)	E_d (eV)	λ_{os} (nm)	S_{os} (m^{-2})	$n_0 \pm 0.01$
100/0	5.40	5.97	230	2.09×10^{13}	1.45
75/25	6.18	5.99	201	2.40×10^{13}	1.40
50/50	6.81	7.73	182	3.43×10^{13}	1.46
25/75	5.59	5.58	222	2.02×10^{13}	1.41
0/100	7.07	6.43	176	2.93×10^{13}	1.38

Full Paper

Effect of γ -irradiation on color detection

The color detection method is one of the several techniques that have been employed to assess the physical and chemical changes in polymers after being mixed with other materials as well as when exposed to γ -irradiation. The color detection method CIE XYZ is internationally recognized and therefore will be used in the present work for the description of colored samples. In this technique, a color is specified by its tristimulus values XYZ depending on the color matching functions of the standard observer defined by CIE^[41].

(a) 75/25 wt/wt% PMMA/PVAc blend sample

The chromaticity coordinates x and y were calculated for 75/25 wt/wt% PMMA/PVAc blend samples irradiated with various γ -dose. Figure 7a shows the position of different irradiated specimens on the chromaticity locus and their distance to the white point. The position of irradiated sample at 20 kGy lies on the left side but nearer to the achromatic point than other irradiated samples. But the locations of the pristine and other irradiated samples are very near to each other; so that they overlap and are represented by a single point on the left side of the achromatic point. This indicates the presence of very small color gradient. TABLE 4a gives the variation of the color parameters (L^* , U^* , V^* , and C^*) for the blend sample of 25 wt% PVAc as a function of γ -dose that was calculated from the transmittance data. The values of U^* , V^* , and C^* increase as the γ -dose increases up to 20 kGy followed by a decrease up to 100 kGy γ -dose. The blend sample irradiated at 20 kGy has the highest values of color parameters (U^* , V^* and C^*). The values of L^* for irradiated samples are nearly equal except at 20 kGy which has the lowest value.

The color differences between the irradiated samples and the pristine one; ΔL^* , ΔU^* , ΔV^* , ΔC^* and ΔE were calculated for all investigated samples and are presented in TABLE 4a. The data in this Table indicate that all irradiated samples are darker except the irradiated sample at 100 kGy which is lighter than the pristine one. The irradiated samples at 10, 20 and 50 kGy γ -dose are more red, more yellow and more saturated than the pristine sample. On the contrary, the irradiated sample at 5 kGy γ -dose is more green, more blue and less saturated than the pristine one. However, the irradiated

sample at 100 kGy γ -dose is more green, more yellow and more saturated than the pristine one. Also, the total color difference ΔE at 20 kGy γ -dose is the highest compared with those of the other irradiated samples. Therefore, it may be assumed that the degree of variation of the color parameters depends mainly on the quantity of γ -radiation received by the material^[42].

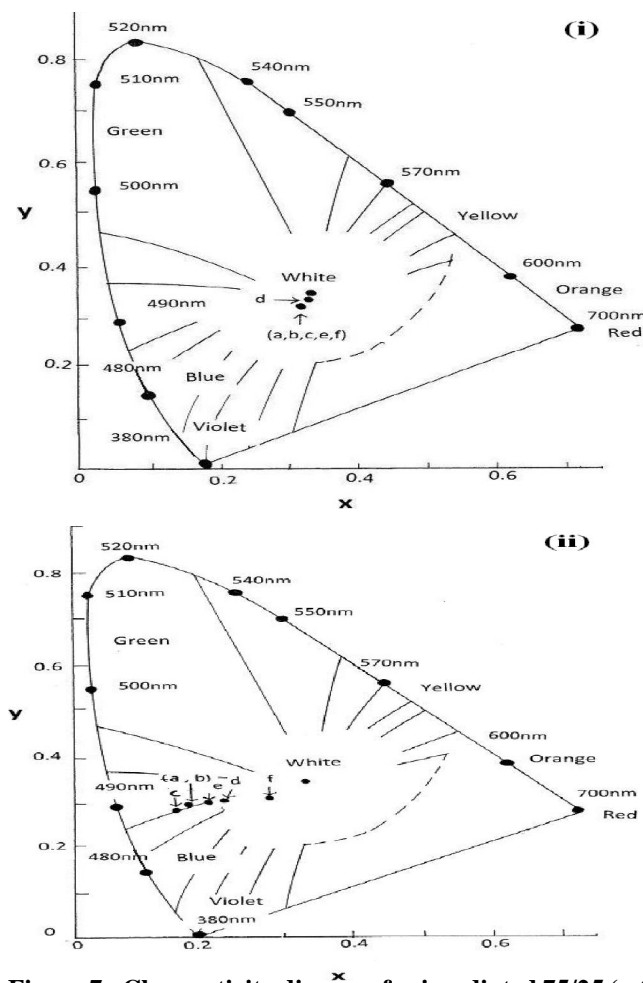


Figure 7 : Chromaticity diagram for irradiated 75/25 (wt/wt%) PMMA/PVAc blend sample undoped (i) and doped with malachite green (ii) at: (a)zero, (b)5, (c)10, (d)20, (e)50 and (f)100 kGy γ -doses

(b) 75/25 wt/wt% PMMA/PVAc blend sample doped with malachite green

The chromaticity coordinates x and y were calculated for pristine and γ -irradiated 75/25 wt/wt% PMMA/PVAc blend samples doped with malachite green at various γ -doses. Figure 7b shows the position of all specimens on the chromaticity locus and their distance to the white point. The positions for the pristine and γ -irradiated blend sample at 5 kGy are identical

and represented by a single point. The pristine and all γ -irradiated blend samples lie on the left side of the achromatic point and within the blue-green region. The distance of each sample position from the white point follows the following sequence at γ -doses 10kGy>5kGy>50kGy>20kGy>100kGy. The results indicate that the γ -irradiated blend samples doped with malachite green has a high color gradient.

TABLE 4b also presents the variation of the color parameters (L^* , U^* , V^* and C^*), calculated from the transmittance data, for 75/25 wt/wt% PMMA/PVAc blend samples doped with malachite green as a function of the γ -dose. It is clear that the changes in the values of L^* , and V^* color parameters are irregular. In addition, the values of U^* and C^* indicate that the greenness and saturation of the pristine and irradiated samples decrease with increasing the γ -dose.

TABLE 4 : The color parameters of pristine and irradiated 75/25 (wt/wt%) PMMA/PVAc blend sample undoped (a) and doped with malachite green (b) at different γ -doses

(A)										
γ -doses. kGy	L^*	U^*	V^*	C^*	ΔL^*	ΔU^*	ΔV^*	ΔC^*	ΔE	
0	95.2	0.36	1.24	1.29	----	----	----	----	---	
5	94.7	0.34	1.04	1.09	-0.5	-0.02	-0.2	-0.2	0.6	
10	94.3	0.40	1.90	1.94	-0.9	0.04	0.7	0.6	1.1	
20	92.8	1.83	8.77	8.96	-2.4	1.47	7.5	7.7	8.0	
50	94.4	0.97	5.29	5.38	-0.8	0.61	4.0	4.1	4.2	
100	95.4	0.33	2.17	2.19	0.2	-0.03	0.9	0.9	0.9	

(B)										
γ -doses. kGy	L^*	U^*	V^*	C^*	ΔL^*	ΔU^*	ΔV^*	ΔC^*	ΔE	
0	62.2	-86.3	-30.6	91.5	-----	-----	-----	-----	-----	
5	58.8	-79.7	-32.4	86.1	-3.5	6.5	-1.8	-5.5	7.6	
10	42.8	-66.1	-32.1	73.2	-19.5	20.1	-16.0	-18.0	28.1	
20	70.7	-60.1	-21.5	63.8	8.4	26.2	9.1	-27.7	28.9	
50	61.2	-55.2	-25.9	60.9	-1.1	31.1	4.7	-30.6	31.4	
100	83.9	-23.1	-10.9	25.6	21.7	63.1	19.6	-65.9	69.6	

C^* (chroma) = $(U^{*2} + V^{*2})^{1/2}$, CIE $L^*U^*V^*$ Differences. ΔL^* is the lightness difference, ΔU^* is the red-green color difference, ΔV^* is the yellow-blue color difference, $\Delta C^* = [(\Delta U^*)^2 + (\Delta V^*)^2]^{1/2}$, $\Delta E = [(\Delta L^*)^2 + (\Delta U^*)^2 + (\Delta V^*)^2]^{1/2}$

The data of color differences between the pristine and the irradiated samples at 5, 10 and 50 kGy γ -doses are darker, while the irradiated samples at 20 and 100 kGy γ -doses are much lighter than the pristine one. All γ -irradiated samples are more red, less saturated and

more yellow except for the γ -irradiated samples at 5, 10 kGy γ -dose where they are more blue than the pristine sample. It must be mentioned also that the total color difference ΔE at 100 kGy γ -dose is the highest when compared to the other irradiated samples.

CONCLUSIONS

A single glass transition temperature for each blend sample was observed from DTA thermogram, which reflects the existence of miscibility in investigated samples. Also, the shift of the absorption bands at 230 and 270 nm for PMMA and PVAc respectively in UV-visible spectra towards a lower wavelength for all blend samples indicates the occurrence of an intermolecular interaction between PMMA and PVAc homopolymers, which support the existence of miscibility of such system. From TGA data it was shown that the addition of 75 wt% PVAc to PMMA exhibits a stabilizing effect due to high molecular weight and the intermolecular cross-linking reaction. The UV-visible spectra revealed that the blend sample of composition 75 wt% PVAc content has a maximum absorbance value in UV wavelength range compared to other blend samples. The enhancement of both thermal stability and absorbance of 75 wt% PVAc content blend sample prefer its uses in many possible medical applications. It was evident that the pristine and γ -irradiated 25 wt% PVAc doped with malachite green blend samples have a highly significant color gradient on the chromaticity diagram compared to counterparts in the undoped blend samples. So, malachite green and γ -irradiation play an important role in the color gradient.

REFERENCES

- [1] A.M.Stephen, T.P.Kumar, N.G.Renganathan, S.Pitchumani, R.Thirunakaran, N.Muniyandi; J.Power Source, **89**, 80 (2000).
- [2] M.Tang, W.R.Liau; Eur.Polym.J., **36**, 2597 (2000).
- [3] K.Pielichowski, I.Harmerton; Eur.Polym.J., **36**, 171 (2000).
- [4] S.M.Pawde, K.Deshmukh; J.of Appl.Polym.Sci., **114**, 2169 (2009).
- [5] F.H.Abd El-kader, S.A.Gaafar, K.H.Mahmoud, S.I.Bannan, M.F.H.Abd El-kader; J.Curr.Appl. Phys., **8**, 78 (2008).

Full Paper

- [6] H.M.Zidan, E.M.Abdelrazek; *Int.J.Polym.Mater.*, **54**, 1073 (2005).
- [7] H.C.Kuan, S.L.Chiu, C.H.Chen, C.F.Kuan, C.L.Chiang; *J.Appl.Polym.Sci.*, **113**, 1959 (2009).
- [8] Z.Guo, G.Yang, Z.Huang, J.Huang; *J.Macromol Rapid Commun.*, **22**, 120 (2001).
- [9] P.Gustafik, O.Sugihara, N.Okamoto; *Jpn.J.Appl. Phys.*, **43**, 2011 (2004).
- [10] E.M.Abdelrazek, G.El-Damrawi, I.S.Elashmawi, A.El-Shahawy; *App.Sur.Sci.*, **256**, 2711 (2010).
- [11] D.L.Mac Adam; *Color measurements theme, variation*, springer, heidelderg, (1981).
- [12] A.K.Adiyodi, X.Joseph, P.V.Jyothy, G.Jose, N.V.Unnikrishnan; *Mater.Sci-Poland.*, **27**, 297 (2009).
- [13] E.G.Crispim, A.F.Rubira, E.C.Muniz; *Polymer*, **40**, 5129 (1999).
- [14] V.Sankar, T.S.Kumar, K.P.Rao; *Trends Biomater.Artif.Organs.*, **17**, 24 (2004).
- [15] B.Serrano, J.Baselga, I.Esteban, L.M.Sese, I.F.Pie'rola; *J.Appl.Polym.Sci.*, **89**, 1284 (2003).
- [16] Y.Tang, J.Scheinbeim; *J.Polym.Sci.Pol.Phys.*, **41**, 927 (2003).
- [17] L.Chang, Y.H.Chou, E.M.Woo; *Colloid Polym.Sci.*, **289**, 199 (2011).
- [18] R.Baskaran, S.Selvasekarapandian, N.Kuwata, Y.Iwai, J.Kawamura, T.Hattori; *J.Appl.Polym.Sci.*, **110**, 1945 (2008).
- [19] W.B.WU, W.Y.Chiu, W.B.Liau; *John Wiley & Sons, Inc.*, ccc0021-8995197/030411-11 (1997).
- [20] T.G.Fox; *Bull.Am.Phys.Soc.*, **1**, 123 (1956).
- [21] B.J.Holland, J.N.Hay; *Polym.Degrad.Stab.*, **77**, 435 (2002).
- [22] Y.M.Lee, D.S.Viswanath; *Polym.Eng.Sci.*, **40**, 2332 (2000).
- [23] E.Kandare, H.Deng, D.Wang, J.M.Hossenlopp; *Polym.Adv.Technol.*, **17**, 312 (2006).
- [24] H.M.Nizam El-Din, A.M.El-Naggar, F.I.Ali; *J.Appl.Polym.Sci.*, **99**, 1773 (2006).
- [25] W.Zhao, Q.Zhang, J.Zhang, H.Zhang; *Polym. Composite*, **30**, 891 (2009).
- [26] H.H.Horowitz, G.Metzger; *Analytical Chemistry*, **35**, 1464 (1963).
- [27] F.Urbach; *Phys.Rev.*, **92**, 1324 (1953).
- [28] N.F.M, E.A.Davis; *Electronic process in non-crystalline materials 2nd Edition*, Oxford University press, Oxford, (1979).
- [29] J.D.Dow, D.Redfield; *Phys.Rev.*, **B5**, 594 (1977).
- [30] M.Zanini, J.Tauc; *Non-Cryst.Solids*, **23**, 349 (1977).
- [31] S.K.JAl-Ani, C.A.Hogarth, R.A.El-Malawany; *J.Mater.Sci.*, **20**, 661 (1985).
- [32] M.Modreanu, M.Gartner, N.Tomozeiu, A.Szekeres; *J.Optoelectron.Adv.M.*, **3**, 575 (2001).
- [33] V.Prajzler, I.Huttel, O.Lyutakov, J.Oswald, V.Machovic, V.Jerabek; *Polym.Eng.Sci.*, 1814 (2009).
- [34] M.Yamaguchi, K.Masuzawa; *Eur.Polym.J.*, **43**, 3277 (2007).
- [35] W.Daniels; *Vinyl ester polymers. In transitions and relaxations to zwitterionic polymerization*, encyclopedia of polymer science and engineering 2nd Edition, H.F.Mark(Ed); *John Wiley & Sons: New York*, **17**, 402 (1987).
- [36] R.M.Ahmed; *Int.J.Photoenergy*, Article ID 150389, (2009).
- [37] H.K.Kim, F.G.Shi; *J.Mater.Sci.Electronics*, **12**, 361 (2001).
- [38] A.F.Qasrawi; *Cryst.Res.Technol.*, **40**, 610 (2005).
- [39] S.H.Wemple; *Phys.Rev.*, **B7**, 3767 (1973).
- [40] N.M.Gasanly; *Cryst.Res.Technol.*, **44**, 322 (2009).
- [41] CIE, *Publication No.15, 2, Colorimetry, 2nd Edition*, Commission Internationale de 'Ec' lairage, Vienna, Austria, (1986).
- [42] W.W.Parkinson; *Encyclopedia of Polymer Science and Technology*, N.M.Bikals, H.F.Mark, N.G.Goylord, (Eds); *John wiely and N.Y.Sons.Inc.*, **2**, (1969).